
Weakly-Supervised Conditional Embedding for Referred Visual Search

Simon Lepage^{1,2} Jérémie Mary¹ David Picard²

¹ CRITEO AI Lab, Paris, France

² LIGM, École des Ponts, Marne-la-Vallée, France

{s.lepage, j.mary}@criteo.com david.picard@enpc.fr

Abstract

This paper presents a new approach to image similarity search in the context of fashion, a domain with inherent ambiguity due to the multiple ways in which images can be considered similar. We introduce the concept of Referred Visual Search (RVS), where users provide additional information to define the desired similarity. We present a new dataset, LAION-RVS-Fashion, consisting of 272K fashion products with 842K images extracted from LAION, designed explicitly for this task. We then propose an innovative method for learning conditional embeddings using weakly-supervised training, achieving a 6% increase in Recall at one (R@1) against a gallery with 2M distractors, compared to classical approaches based on explicit attention and filtering. The proposed method demonstrates robustness, maintaining similar R@1 when dealing with 2.5 times as many distractors as the baseline methods. We believe this is a step forward in the emerging field of Referred Visual Search both in terms of accessible data and approach¹.

1 Introduction

Image embeddings generated by deep neural networks play a crucial role in a wide range of computer vision tasks. Image retrieval, in particular, has gained substantial prominence, leading to the development of dedicated vector database systems[23]. These systems facilitate efficient search and retrieval by comparing embedding values and identifying the most similar images within the database.

Image similarity search in the context of fashion presents a unique challenge due to the inherently ill-founded nature of the problem. The primary issue arises from the fact that two images can be considered similar in various ways, leading to ambiguity in defining a single similarity metric. For instance, two images of clothing items may be deemed similar based on their color, pattern, style, or even the model pictured. This multifaceted nature of similarity in fashion images complicates the task of developing a universally applicable similarity search algorithm, as it must account for these various ways in which images can be related.

A natural idea is to ask users to provide additional information explaining what they are interested in, for example providing a picture of a person and indicating interest in the hat. We propose to name this task Referred Visual Search (RVS), as it is poised to gain interest in the computer vision community because of the product search in large catalogs.

In practice, object selection in complex scenes is classically tackled using object detection and crops [22, 17, 12, 41]. Some recent approaches use categorical attributes [7] or text instead [5], and automatically crop the image based on attention to input attributes. Recently, Jiao et al. [21] made a step further, incorporating prior knowledge about the taxonomy of fashion attributes and classes without using crops. They are using a multi-granularity loss and two sub-networks to learn attribute

¹Code, data and models are available at <https://github.com/Simon-Lepage/CondViT-LRVSF>

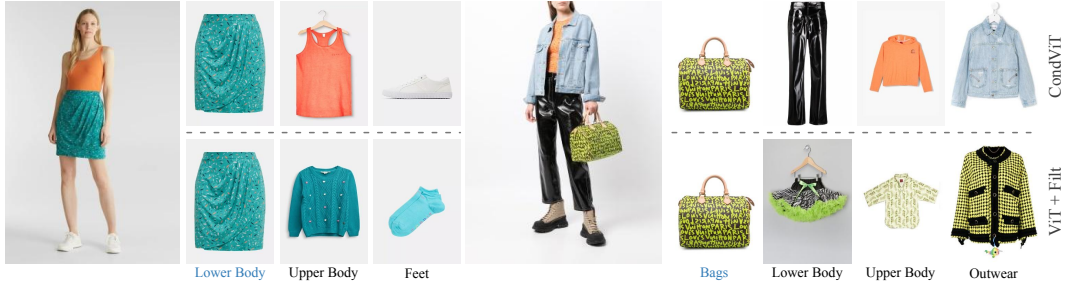


Figure 1 – Qualitative comparison on samples from the LRVS-F test set. The scenes are used as queries, while the products are top-1 retrieval in our gallery, for different categories. The default category associated with the scene is in blue. Our Conditional ViT (first row) can dynamically extract features for various objects, while an unconditional baseline with filtering (second row) fails to capture relevant features from non-salient objects.

and class-specific representations, resulting in improved robustness for fashion retrieval, yet without providing any code or dataset. In this work, we aim to continue in this direction and totally eliminate the need for explicit detection or segmentation while still producing similarities in the embedding space specific to the conditioning. Indeed, all approaches resorting to segmentation require multiple embedding computations when facing a complex image (*i.e.*, containing multiple objects of interest). To our knowledge, no public dataset is available for this task. Therefore and to demonstrate the soundness of our approach, we extracted a subset of LAION 5B focused on pairs of images sharing a labeled similarity in the domain of Fashion.

This paper presents two contributions to the emerging field of Referred Visual Search, aiming at defining image similarity based on conditioning information.

- ✓ The introduction of a new dataset, referred to as LAION-RVS-Fashion, which is derived from the LAION 5B dataset and comprises 272K fashion products with nearly 842K images. This dataset features a test set with an addition of more than 2M distractors, enabling the evaluation of method robustness in relation to gallery size. The dataset’s pairs and additional metadata are designed to necessitate the extraction of particular features from complex images.
- ✓ An innovative method for learning to extract referred embeddings using weakly-supervised training. Our approach demonstrates superior accuracy compared to the baseline, achieving an 6% increase in R@1 against 2M distractors. Furthermore, our method exhibits robustness against a large number of distractors, maintaining high R@1 even when increasing the number of distractors by 2.5 times.

2 Related Work

Multi-modal Models. Deep learning has made significant progress in both vision and language domains, leading to the emergence of new vision-language methods. This new field notably developed Vision-Language Pre-Training [10], leveraging many pretext tasks to create models that can be finetuned for downstream multi-modal applications. Specific models have been trained on fashion datasets to extract more relevant features [61, 36, 13, 20], and applied to multi-modal product retrieval [57, 52, 60]. In our work, we use CLIP [40] as a general feature extractor for our visual encoder.

Vision-Language processing also brought new challenges, in particular Referring Expression Comprehension and Segmentation where a sentence designates an object in a scene, that the network has to localize. For the comprehension task (similar to open-vocabulary object detection) the goal is to output a bounding box [34, 54, 55, 30]. The segmentation task aims at producing an instance mask for images [59, 34, 19, 6, 25] and recently videos [50, 3]. In this paper, we propose a new referring expression task, where the goal is to embed the object of interest into a representation that can be used for retrieval.

Instance Retrieval. In the last decade, content-based image retrieval has changed because of the arrival of deep learning, which replaced many handcrafted heuristics (keypoint extraction, descriptors,

geometric matching, re-ranking. . .) [11]. In the industry this technology has been of interest to retail companies and search engines to develop visual search solutions, with new challenges stemming from the large scale of such databases. Initially using generic pretrained backbones to extract embeddings with minimal retraining [51], methods have progressively evolved toward domain-specific embeddings supervised by semantic labels, and then multi-task domain-specific embeddings, leveraging additional product informations [56, 2, 45]. The latest developments in the field incorporate multi-modal features for text-image matching [57, 52, 60], with specific vision-language pretext tasks.

However, these methods often consider that the query image is unambiguous, and often rely on a region proposal system to crop the initial image [22, 58, 17, 41, 2, 9]. In our work, we remove this heuristic and propose an end-to-end framework, leveraging the Transformer architecture to implicitly perform this detection step conditionally to the query text.

Conditional Embeddings. Conditional similarity search has been attempted in two ways: by modifying the retrieval process or the embedding process. On one hand, for the retrieval process, Hamilton et al. [15] propose to use a dynamically pruned random projection tree. On the other hand, for the embeddings, previous work in conditional visual similarity learning has been oriented toward attribute-specific retrieval, considering that different similarity spaces should be defined depending on chosen discriminative attributes [46, 37]. These approaches use either a mask applied on the features [46], or different projection heads [37], and require extensive data labeling.

In Fashion, ASEN [35] uses spatial and channel attention to an attribute embedding to extract specific features in a global branch. Dong et al. [7] and Das et al. [5] build upon this model and add a local branch working on an attention-based crop. Recently, Jiao et al. [21] incorporated prior knowledge about fashion taxonomy in this process to create class-conditional embeddings based on known fine-grained attributes, using multiple attribute-conditional attention modules. In our work, we use Vision Transformers [8] to implicitly pool features depending on the conditioning information, without relying on explicit ROI cropping or labeled fine-grained attributes.

A form of conditional retrieval can also be seen in the dialog-based interactive retrieval setting, where an image query is iteratively refined following user instructions [14, 49, 53, 16]. Close to our work although in a different domain, Asai et al. [1] tackle a conditional document retrieval task, where the user intent is made explicit by concatenating instructions to the query documents.

Retrieval Datasets. Standard datasets in metric learning literature consider that the images are object-centric, and focus on single salient objects [44, 47, 26]. In the fashion domain there exist multiple datasets dedicated to product retrieval, with paired images depicting the same product and additional labeled attributes. A recurrent focus of such datasets is cross-domain retrieval, where the goal is to retrieve images of a given product taken in different situations, for exemple consumer-to-shop [31, 48, 32, 12], or studio-to-shop [28, 32]. The domain gap is in itself a challenge, with issues stemming from irregular lighting, occlusions, viewpoints, or distracting backgrounds. However, the query domain (consumer images for exemple) often contains scenes with multiple objects, making queries ambiguous. This issue has been circumvented with the use of object detectors and landmarks detectors [24, 32, 12, 18]. Some of these datasets are not accessible anymore [24, 32, 48].

With more than 272k distinct training product identities captured in multi-instance scenes, our new dataset proposes an exact matching task similar to the private Zalando dataset [28], while being larger than existing fashion retrieval datasets in addition to being publicly available. We also create an opportunity for new multi-modal approaches, with captions referring to the product of interest in each complex image, and for robustness to gallery size with 2M added distractors at test time.

3 Conditional Embedding

Task Formulation: Let x_q be a query image, and c_q associated referring information. Similarly, let x_t be a target image, described by the latent information c_t . Both c_q and c_t can be thought of as categories or textual referring information. The probability of x_t to be relevant for the query x_q is given by the conditional probability $P(x_t, c_t|x_q, c_q)$. When working with categories, a filtering strategy consists in assuming independence between the images and their category,

$$P(x_t, c_t|x_q, c_q) = P(x_t|x_q)P(c_t|c_q), \tag{1}$$

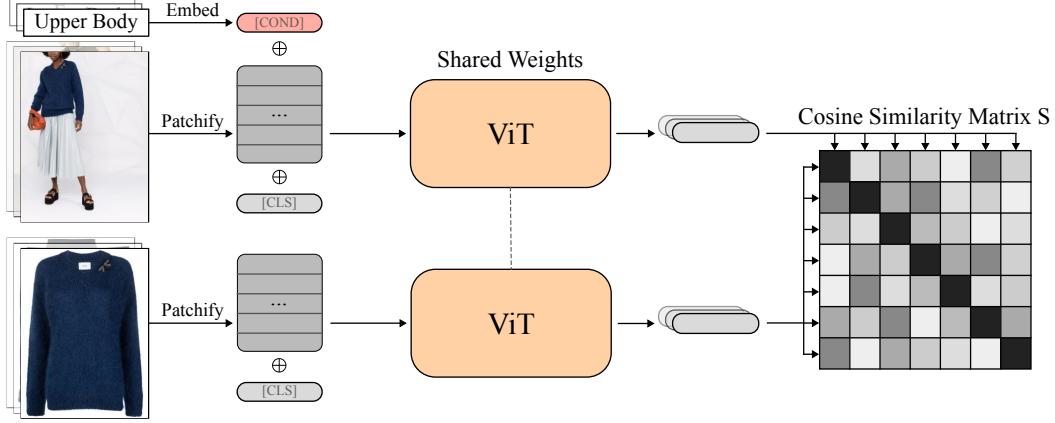


Figure 2 – Overview of our method on LRVS-F. For each element in a batch, we embed the scene conditionally and the isolated item unconditionally. We optimize a Normalized Temperature-scaled Cross Entropy loss over the cosine similarity matrix. \oplus denotes concatenation to the patch sequence.

and further assuming that categories are uncorrelated (i.e., $P(c_t|c_q) = \delta_{c_q=c_t}$ with δ the Dirac distribution). In this work, we remove those assumptions and instead assume that $P(x_t, c_t|x_q, c_q)$ can be directly inferred by a deep neural network model. More specifically, we propose to learn a flexible embedding function ϕ such that

$$\langle \phi(x_q, c_q), \phi(x_t, c_t) \rangle \propto P(x_t, c_t|x_q, c_q). \quad (2)$$

Our approach offers a significant advantage by allowing the flexibility to change the conditioning information (c_q) at query time, enabling a focus on different aspects of the image.

Method: We implement ϕ by modifying the vision transformer architecture [8]. The conditioning is an additional input token with an associated learnable positional encoding, concatenated to the sequence of image patches. The content of this token can either be learned directly (e.g. for discrete categorical conditioning), or be generated by another network (e.g. for textual conditioning). We experimented with concatenating at different layers in the transformer, and found that concatenating before the first layer is the most sensible choice (see Appendix B.3). At the end of the network, we apply a linear projection to the [CLS] token to map the features to a metric space.

We compute the similarity between two embeddings $z_i = \phi(x_i, c_i), z_j = \phi(x_j, c_j) \in \mathbb{R}^d$ with the cosine similarity $s(z_i, z_j) = z_i^\top z_j / (\|z_i\| \|z_j\|)$. In practice we normalize the embeddings to the hypersphere at the end of the network, and use simple inner products during training and retrieval.

We train the network with Normalized Temperature-scaled Cross Entropy Loss (NT-Xent) [4, 43], using the same variation as CLIP [40], which is detailed in the next paragraph. However, we hypothesize that even though our method relies on a contrastive loss, it does not explicitly require a specific formulation of it. We choose the NT-Xent loss because of its popularity and scalability.

During training, given a batch of N pairs of images and conditioning $((x_i^A, c_i^A); (x_i^B, c_i^B))_{i=1..N}$, we compute their conditional embeddings $(z_i^A, z_i^B)_{i=1..N}$, and a similarity matrix S where $S_{ij} = s(z_i^A, z_j^B)$. We then optimize the cosine similarity of the correct pair with a cross-entropy loss, effectively considering the $N - 1$ other products in the batch as negatives:

$$l(S) = -\frac{1}{N} \sum_{i=1}^N \log \frac{\exp(S_{ii}\tau)}{\sum_{j=1}^N \exp(S_{ij}\tau)}, \quad (3)$$

with τ a learned temperature parameter, and the final loss is $\mathcal{L} = l(S)/2 + l(S^\top)/2$. Please refer to Fig. 2 for an overview of the method.

At test time, we use FAISS [23] to create a unique index for the entire gallery and perform fast similarity search on GPUs.



Figure 3 – Samples from LRVS-F. Each product is represented on at least a simple and a complex image, and is associated with a category. The simple images are also described by captions from LAION and BLIP2. Please refer to Appendix A.1 for more samples.

4 Dataset

Metric learning methods work by extracting features that pull together images labeled as similar [11]. In our case, we wanted to create a dataset where this embedding has to focus on a specific object in a scene to succeed. We found such images in fashion, thanks to a standard practice in this field consisting in taking pictures of the products alone on neutral backgrounds, and worn by models in scenes involving other clothing items (see Fig. 3).

We created LAION-RVS-Fashion (abbreviated LRVS-F) from LAION 5B by collecting images of products isolated and in context, which we respectively call *simple* and *complex*. We grouped them using extracted product identifiers. We also gathered and created a set of metadata to be used as referring information, namely LAION captions, generated captions, and generated item categories. Details about these metadata are given in 4.1, and statistics in Appendix A.2.

In total, we extracted 272,451 products for training, represented in 841,718 images. This represents 581,526 potential simple/complex positive pairs. We additionally extracted 400 products (800 images) to create a validation set, and 2,000 products (4,000 images) for a test set. We added 99,541 simple images in the validation gallery as distractors, and 2,000,014 in the test gallery. Details about the benchmark will be given in section 4.2.

4.1 Construction

Image Collection: The raw data of LRVS-F are collected from a list of fashion brands and retailers whose content delivery network domains were found in LAION 5B. We used the automatically translated versions of LAION 2B MULTI and LAION 1B NOLANG to get english captions for all the products. This represents around 8M initial images.

We analyzed the format of the URLs for each domain, and extracted image and product identifiers using regular expressions when possible. We removed duplicates at this step using these identifiers, and put aside images without clear identifiers to be filtered and used as distractors later.

Image Annotation: The additional metadata that we provide were generated using deep learning models. We generated indicators of the image complexity, classified the products in 11 categories, and added new image captions.

First, we used a model to classify the complexity of the images, trained with active learning. We started by automatically labeling a pool of images using information found in the URLs, before manually filtering the initial data, and splitting between training and validation. Then, we computed and stored the pre-projection representations extracted by OpenCLIP B16 for each image, and trained a 2-layers MLP to predict the category. After training, we randomly sampled 1000 unlabeled images and annotated the 100 with the highest prediction entropy, before splitting them between training and validation data. We repeated these 2 steps until reaching over 99% accuracy and labeled the entire dataset using this model.

We used a second model to automatically assign categories to the simple images. LAION captions are noisy, so instead of using them we used BLIP2 FlanT5-XL [29] to answer the question "In one word, what is this object?". We gathered all the nouns from the answers, using POS tagging when the generated answer was longer, and grouped them in 11 categories (10 for clothing, 1 for non-clothing). We automatically created an initial pool of automatically labeled data, which we manually filtered, before applying the same active learning process as above. We then annotated all the simple images with this model. Please refer to Appendix A.2 for the list of categories and their composition.

Finally, we automatically added new descriptions to the simple images, because the quality of some LAION texts was low. For example, we found partially translated sentences, or product identifiers. We generated 10 captions for each image using BLIP2 FlanT5-XL with nucleus sampling, and kept the two with largest CLIP similarity.

Dataset Split: We grouped together images associated to the same product identifier and dropped the groups that did not have at least a simple and a complex image. We manually selected 400 of them for the validation set, and 2,000 for the test set. The distractors are all the images downloaded previously that were labeled as "simple" but not used in product groups. This mostly includes images for which it was impossible to extract any product identifier.

Finally, we used Locally Sensitive Hashing (LSH) with perceptual hash, and OpenCLIP B16 embeddings to remove duplicates. We created FAISS indexes based respectively on hamming distance and cosine similarity, automatically removing samples with extremely high similarity. We manually inspected samples near the threshold. We used this process on complex images from the training set to remove products duplicates, on train and test sets to reduce evaluation bias, and on gallery images and distractors for both the validation and test sets.

4.2 Benchmark

We define a benchmark on LRVS-F to evaluate different methods on a held-out test set with a large number of distractors. The test set contains 2,000 unseen products, and up to 2M distractors. Each product in the set is represented by a pair of images - a simple one and a complex one. The objective of the retrieval task is to retrieve the simple image of each product from among a vast number of distractors and other simple test images, given the complex image and conditioning information.

For this dataset, we propose to frame the benchmark as an asymmetric task : the representation of simple images (the gallery) should not be computed conditionally. This choice is motivated by three reasons. First, when using precise free-form conditioning (such as LAION texts, which contain hashed product identifiers and product names) a symmetric encoding would enable a retrieval based solely on this information, completely disregarding the image query. Second, for discrete (categorical) conditioning it allows the presence of items of unknown category in the gallery, which is a situation that may occur in distractors. Third, these images only depict a single object, thus making referring information unnecessary. A similar setting is used by Asai et al. [1].

Additionally, we provide a list of subsets sampled with replacement to be used for bootstrapped estimation of confidence intervals on the metrics. We created 10 subsets of 1000 test products, and 10 subsets of 10K, 100K and 1M distractors.

We also propose a validation set of 400 products with nearly 100K other distractors to monitor the training and for hyperparameter search.

5 Experiments

Besides implementation details we conduct experiments on referred search conditioning either on category or on text.

5.1 Implementation details

All our models take as input images of size 224×224 , and output an embedding vector of 512 dimensions. We use CLIP weights as initialization, and then train our models for 30 epochs with AdamW [33] and a maximum learning rate of 10^{-5} determined by a learning rate range test [42]. To avoid distorting pretrained features [27], we start by only training the final projection and new input

Distractors →	+0		+10K		+100K		+1M		+2M	
Model	%R@1	%Cat@1	%R@1	%Cat@1	%R@1	%Cat@1	%R@1	%Cat@1	%R@1	%Cat@1
ASEN [7]	73.0 ±1.82	83.9 ±1.10	52.7 ±1.35	69.0 ±1.14	34.3 ±1.73	60.0 ±0.87	20.1 ±1.06	55.1 ±1.36	14.6	53.8
ASEN + Filt. [7]	83.0 ±1.45	-	64.9 ±1.83	-	45.2 ±1.86	-	27.8 ±1.40	-	21.2	-
ASEN _g [7]	79.6 ±1.07	87.1 ±1.05	63.1 ±1.50	76.3 ±1.26	46.1 ±1.21	68.5 ±0.84	29.8 ±1.86	62.9 ±1.27	24.1	62.0
ASEN _g + Filt. [7]	87.7 ±1.01	-	73.6 ±1.39	-	56.1 ±1.14	-	38.6 ±2.20	-	31.2	-
B/32										
CLIP [40]	27.4 ±1.72	65.0 ±1.91	14.6 ±1.24	63.3 ±2.31	6.2 ±1.14	61.2 ±0.83	2.5 ±0.45	58.6 ±1.59	1.5	57.5
CLIP + Filt. [40]	34.9 ±2.19	-	17.4 ±1.63	-	7.4 ±1.30	-	2.8 ±0.51	-	1.7	-
ViT	93.5 ±0.72	96.8 ±0.42	85.6 ±1.08	93.7 ±0.31	73.4 ±1.35	90.9 ±0.78	58.5 ±1.37	87.8 ±0.86	51.7	86.9
ViT + Filt.	95.9 ±0.63	-	88.9 ±1.01	-	76.8 ±1.24	-	62.0 ±1.31	-	55.1	-
CondViT - Categories	97.0 ±0.57	100 ±0.07	90.9 ±0.98	99.2 ±0.31	80.2 ±1.55	98.8 ±0.39	65.8 ±1.42	98.4 ±0.65	59.0	98.0
CondViT - Text	98.2 ±0.46	99.9 ±0.11	92.7 ±0.77	99.1 ±0.30	82.8 ±1.22	98.7 ±0.40	68.4 ±1.50	98.1 ±0.43	62.1	98.0
B/16										
CLIP [40]	38.6 ±1.61	69.5 ±1.62	23.9 ±1.17	68.5 ±1.98	12.6 ±0.97	66.1 ±1.14	6.4 ±0.65	64.1 ±1.01	4.8	63.3
CLIP + Filt. [40]	46.0 ±1.69	-	27.1 ±1.55	-	14.0 ±1.14	-	7.1 ±0.70	-	5.1	-
ViT	94.1 ±0.49	96.9 ±0.42	88.4 ±0.88	94.8 ±0.52	79.0 ±1.02	92.3 ±0.73	66.1 ±1.21	90.2 ±0.92	59.4	88.8
ViT + Filt.	96.1 ±0.64	-	90.9 ±0.88	-	81.9 ±0.87	-	68.9 ±1.11	-	62.4	-
CondViT - Categories	97.7 ±0.21	99.8 ±0.12	93.3 ±1.04	99.5 ±0.25	85.6 ±1.06	99.2 ±0.35	74.2 ±1.82	99.0 ±0.42	68.4	98.8
CondViT - Text	98.2 ±0.33	99.9 ±0.16	94.3 ±0.81	99.4 ±0.40	86.5 ±1.17	98.9 ±0.44	74.2 ±1.63	98.5 ±0.54	69.3	98.4

Table 1 – Comparison of our models to the baselines on LRV5-F benchmark. For 0, 10K, 100K and 1M distractors, we report bootstrapped means and standard deviations estimated from 10 randomly sampled sets. We also report results on the full set of test products and distractors. ASEN_g denotes an ASEN model using only the global branch, in the first stage of the training. Bold results indicate significant improvement ($\geq 2\sigma$) over the corresponding ViT+Filtering.

embeddings (conditioning and positional) for a single epoch, with a linear warm-up schedule. We then train all parameters for the rest of the epochs with a cosine schedule.

We pad the images to a square with white pixels, before resizing the largest side to 224 pixels. During training, we apply random horizontal flip, and random resized crops covering at least 80% of the image area. We evaluate the recall at 1 (R@1) of the model on the validation set at each epoch, and report test metrics (recall and categorical accuracy) for the best performing validation checkpoint.

We used mixed precision and sharded loss to run our experiments on multiple GPUs. B/32 models were trained for 6 hours on 2 V100 GPUs, with a total batch size of 360. B/16 were trained for 9 hours on 12 V100, with a batch size of 420. Batch sizes were chosen to maximize GPU memory use.

5.2 Categorical Conditioning

Baselines: We compare our method with its unconditional equivalents, *i.e.*, CLIP-pretrained ViTs finetuned on our dataset. To account for the additional conditioning information used in our method, we propose to evaluate these models on filtered indexes, containing only items from the category of interest. We do not try to predict the item of interest from the input picture, and instead consider it as a part of the query. We also report metrics before the finetuning process, for reference.

We report the results of the baselines in Table 1. With CLIP features, before finetuning, we observe that despite relatively high categorical accuracy the recall quickly falls below 5%. Filtering helps for small amounts of distractors, but becomes ineffective for larger galleries. This shows that the retrieved items are semantically consistent with the query, but that the features are not specific enough for *instance* retrieval.

With finetuned models, we observe a high Top-1 categorical accuracy (over 86%) even with multiple objects in most of the query images. This accuracy sees a drop of 10% across the tested range of distractors quantities. The ViT-B/16 model reaches 59.4%R@1 for 2M distractors, showing that finetuning the model on paired data helps learning features that are discriminative at the instance level. Filtering the gallery brings a modest mean gain of 2 – 4%R@1 across all quantities of distractors (Fig. 4b), reaching 62.4%R@1 for 2M distractors with a ViT-B/16 architecture. In practice, this approach is impractical as it requires computing and storing an index for each category to ensure consistent number of retrieved items.

However, a qualitative assessment of filtered results exposes undesirable behaviors (Fig. 5). When filtering on a category that does not correspond to the network focus, we observe that the results exhibit colors and textures belonging to the automatically focused object and not the selected one. It shows the embedding does not contain features of multiple objects, which makes filtering irrelevant.

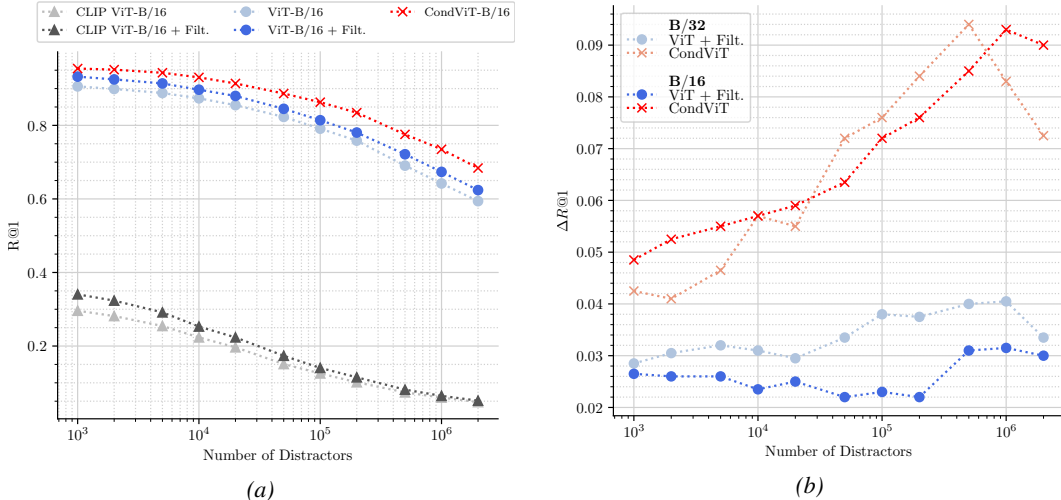


Figure 4 – (a) R@1 with respects to number of added distractors, evaluated on the entire test set. Please refer to Table 1 for bootstrapped metrics and confidence intervals. (b) Difference of R@1 of CondViT and ViT+Filtering with their respective unconditional ViT baseline (B/16 or B/32) against the number of distractors. Filtering brings constant and moderate gains (2 – 4%), whereas conditional embeddings obtain increased performances with the addition of more distractors.

We also compare our results with ASEN [7], trained on our dataset using code released by the authors. This conditional architecture uses a global and a local branch with conditional spatial attention modules, respectively based on ResNet50 and ResNet34 backbones, with explicit ROI cropping. However in our experiments the performances decrease with the addition of the local branch in the second training stage, even after tuning the hyperparameters. The categorical accuracy is similar to that of the untrained CLIP models, and the R@1 benefits from the filtering step.

Conditional ViT: We train our CondViT using the categories provided in our dataset, learning an embedding vector for each of the 10 clothing categories. For the i -th product in the batch, we randomly select in the associated data a simple image x_s and its category c_s , and a complex image x_c . We then compute their embeddings $z_i^A = \phi(x_c, c_s)$, $z_i^B = \phi(x_s)$. We also experimented with symmetric conditioning, using a learned token for the gallery side (see Appendix B.3).

We report the results of our conditional models in Fig. 4a. We observe that the rate of decay of the recall is different, which brings increasing gains relatively to the unconditional models as the number of distractors increases. The performance of the filtered ViT-B/16 baseline is comparable to our CondViT-B/16 with 2.5 times as many distractors. We remark that the categorical accuracy of these models is very high, and does not suffer from the addition of distractors (less than 2% drop with 2M distractors), which completely removes the need for filtering.

A qualitative assessment of the conditional model shows on Fig. 5 its ability to extract relevant features relative to different objects in the scene. This observation holds for objects that are not particularly salient, cropped, or partially occluded. We do observe failure cases for infrequent classes, such as *Waist* or *Hands*. Please refer to Appendix B.1 for more qualitative results, and to Appendix B.2 for attention comparison with ASEN, and PCA plots following Oquab et al. [39].

Interestingly, we observe that our CondViT-B/32 is comparable to the ViT-B/16 models while having a lower computational cost, and the capacity to adapt to a new conditioning a test time.

5.3 Textual conditioning

To further validate our approach, we replace the categorical conditioning with referring expressions, using our generated BLIP2 captions embedded by a Sentence T5-XL model [38]. We chose this model because it embeds the sentences in a 768-dimensional vector, allowing us to simply replace the categorical token. We pre-compute the caption embeddings, and randomly use one of them instead of the product category at training time. At test time, we use the first caption.



Figure 5 – Comparison of product retrieval for different methods. For each query we show the top-1 result in our test gallery with 2M distractors for different categories. For the unconditional ViT, features of the salient object are relevant, but filtering does not generalize to new queries. For ASEN_g, conditioning and filtering help extracting different features, but their quality is low. Our CondViT allows a mix of both, with dynamically extracted relevant features.

In Tab. 1, we observe a gain of 3.1%R@1 for the CondViT-B/32 architecture, and 0.9%R@1 for CondViT-B/16, compared to categorical conditioning against 2M distractors, most likely due to the additional details in the conditioning sentences. When faced with users, this method allows for more natural querying, with free-form referring expressions. Qualitative results are in Appendix B.1.

6 Conclusion & Limitations

We presented a novel approach to image similarity in fashion called Referred Visual Search (RVS), which introduces two significant contributions. Firstly, we introduced the LAION-RVS-Fashion dataset, comprising 272K fashion products and 842K images. Secondly, we proposed a weakly-supervised learning method for extracting referred embeddings. Our approach outperforms the baseline, achieving a 6% increase in R@1 against 2M distractors. These contributions offer valuable resources and techniques for advancing image retrieval systems in the fashion industry and beyond.

However, one limitation of our approach is that modifying the text description to refer to something not present or not easily identifiable in the image does not work effectively. For instance, if the image shows a person carrying a green handbag, a refined search with "red handbag" as a condition would only retrieve a green handbag. The system may also ignore the conditioning if the desired item is small or absent in the database. Examples of such failures are illustrated in Appendix B.4. Additionally, extending the approach to more verticals would be relevant. The broader impact of this research is similar to other works on retrieval, with the significant advantage of producing embeddings that conceal information about personal identity and other undesired elements thanks to the conditioning.

References

- [1] Akari Asai, Timo Schick, Patrick Lewis, Xilun Chen, Gautier Izacard, Sebastian Riedel, Hannaneh Hajishirzi, and Wen-tau Yih. Task-aware retrieval with instructions. *arXiv preprint arXiv:2211.09260*, 2022. 3, 6
- [2] Sean Bell, Yiqun Liu, Sami Alsheikh, Yina Tang, Edward Pizzi, M. Henning, Karun Singh, Omkar Parkhi, and Fedor Borisjuk. GrokNet: Unified Computer Vision Model Trunk and Embeddings For Commerce. In *Proceedings of the 26th ACM SIGKDD International Conference on Knowledge Discovery & Data Mining*, pages 2608–2616. ACM, August 2020. ISBN 978-1-4503-7998-4. doi: 10.1145/3394486.3403311. 3
- [3] Adam Botach, Evgenii Zheltonozhskii, and Chaim Baskin. End-to-end referring video object segmentation with multimodal transformers. In *Proceedings of the IEEE/CVF Conference on Computer Vision and Pattern Recognition (CVPR)*, pages 4985–4995, June 2022. 2
- [4] Ting Chen, Simon Kornblith, Mohammad Norouzi, and Geoffrey Hinton. A simple framework for contrastive learning of visual representations. In *International conference on machine learning*, pages 1597–1607. PMLR, 2020. 4
- [5] Nilotpal Das, Aniket Joshi, Promod Yenigalla, and Gourav Agrwal. MAPS: Multimodal Attention for Product Similarity. *Proceedings of the IEEE/CVF Winter Conference on Applications of Computer Vision (WACV)*, pages 3338–3346, 2022. 1, 3
- [6] Henghui Ding, Chang Liu, Suchen Wang, and Xudong Jiang. Vision-Language Transformer and Query Generation for Referring Segmentation. In *2021 IEEE/CVF International Conference on Computer Vision (ICCV)*, pages 16301–16310. IEEE, October 2021. ISBN 978-1-66542-812-5. doi: 10.1109/ICCV48922.2021.01601. 2
- [7] Jianfeng Dong, Zhe Ma, Xiaofeng Mao, Xun Yang, Yuan He, Richang Hong, and Shouling Ji. Fine-Grained Fashion Similarity Prediction by Attribute-Specific Embedding Learning. *IEEE Transactions on Image Processing*, 30:8410–8425, 2021. ISSN 1057-7149, 1941-0042. doi: 10.1109/TIP.2021.3115658. 1, 3, 7, 8
- [8] Alexey Dosovitskiy, Lucas Beyer, Alexander Kolesnikov, Dirk Weissenborn, Xiaohua Zhai, Thomas Unterthiner, Mostafa Dehghani, Matthias Minderer, Georg Heigold, Sylvain Gelly, Jakob Uszkoreit, and Neil Houlsby. An image is worth 16x16 words: Transformers for image recognition at scale. In *International Conference on Learning Representations*, 2021. 3, 4
- [9] Ming Du, Arnau Ramisa, Amit Kumar K C, Sampath Chanda, Mengjiao Wang, Neelakandan Rajesh, Shasha Li, Yingchuan Hu, Tao Zhou, Nagashri Lakshminarayana, Son Tran, and Doug Gray. Amazon Shop the Look: A Visual Search System for Fashion and Home. In *Proceedings of the 28th ACM SIGKDD Conference on Knowledge Discovery and Data Mining*, pages 2822–2830. ACM, August 2022. ISBN 978-1-4503-9385-0. doi: 10.1145/3534678.3539071. 3
- [10] Yifan Du, Zikang Liu, Junyi Li, and Wayne Xin Zhao. A Survey of Vision-Language Pre-Trained Models. *Proceedings of the Thirty-First International Joint Conference on Artificial Intelligence*, 2022. 2
- [11] Shiv Ram Dubey. A Decade Survey of Content Based Image Retrieval using Deep Learning. *IEEE Transactions on Circuits and Systems for Video Technology*, 32(5):2687–2704, May 2022. ISSN 1051-8215, 1558-2205. doi: 10.1109/TCSVT.2021.3080920. 3, 5
- [12] Yuying Ge, Ruimao Zhang, Xiaogang Wang, Xiaoou Tang, and Ping Luo. DeepFashion2: A Versatile Benchmark for Detection, Pose Estimation, Segmentation and Re-Identification of Clothing Images. In *2019 IEEE/CVF Conference on Computer Vision and Pattern Recognition (CVPR)*, pages 5332–5340. IEEE, June 2019. ISBN 978-1-72813-293-8. doi: 10.1109/CVPR.2019.00548. 1, 3
- [13] Sonam Goenka, Zhaoheng Zheng, Ayush Jaiswal, Rakesh Chada, Yue Wu, Varsha Hedau, and Pradeep Natarajan. FashionVLP: Vision Language Transformer for Fashion Retrieval with Feedback. In *2022 IEEE/CVF Conference on Computer Vision and Pattern Recognition (CVPR)*, pages 14085–14095. IEEE, June 2022. ISBN 978-1-66546-946-3. doi: 10.1109/CVPR52688.2022.01371. 2
- [14] Xiaoxiao Guo, Hui Wu, Yu Cheng, Steven Rennie, Gerald Tesaro, and Rogerio Feris. Dialog-based Interactive Image Retrieval. In *Advances in Neural Information Processing Systems*, volume 31. Curran Associates, Inc., 2018. 3
- [15] Mark Hamilton, Stephanie Fu, Mindren Lu, Johnny Bui, Darius Bopp, Zhenbang Chen, Felix Tran, Margaret Wang, Marina Rogers, Lei Zhang, Chris Hoder, and William T. Freeman. MosAIC: Finding Artistic Connections across Culture with Conditional Image Retrieval. In *Proceedings of the NeurIPS 2020 Competition and Demonstration Track*, pages 133–155. PMLR, August 2021. 3

- [16] Xiao Han, Sen He, Li Zhang, Yi-Zhe Song, and Tao Xiang. UIGR: Unified Interactive Garment Retrieval. In *Proceedings of the IEEE/CVF Conference on Computer Vision and Pattern Recognition*, April 2022. 3
- [17] Houdong Hu, Yan Wang, Linjun Yang, Pavel Komlev, Li Huang, Xi Chen, Jiawei Huang, Ye Wu, Meenaz Merchant, and Arun Sacheti. Web-scale responsive visual search at bing. In *Proceedings of the 24th ACM SIGKDD international conference on knowledge discovery & data mining*, pages 359–367, 2018. 1, 3
- [18] Junshi Huang, Rogerio Feris, Qiang Chen, and Shuicheng Yan. Cross-Domain Image Retrieval with a Dual Attribute-Aware Ranking Network. In *2015 IEEE International Conference on Computer Vision (ICCV)*, pages 1062–1070. IEEE, December 2015. ISBN 978-1-4673-8391-2. doi: 10.1109/ICCV.2015.127. 3
- [19] Shaofei Huang, Tianrui Hui, Si Liu, Guanbin Li, Yunchao Wei, Jizhong Han, Luoqi Liu, and Bo Li. Referring Image Segmentation via Cross-Modal Progressive Comprehension. In *2020 IEEE/CVF Conference on Computer Vision and Pattern Recognition (CVPR)*, pages 10485–10494. IEEE, June 2020. ISBN 978-1-72817-168-5. doi: 10.1109/CVPR42600.2020.01050. 2
- [20] Ge-Peng Ji, Mingchen Zhuge, Dehong Gao, Deng-Ping Fan, Christos Sakaridis, and Luc Van Gool. Masked vision-language transformer in fashion. *Machine Intelligence Research*, February 2023. 2
- [21] Yang (Andrew) Jiao, Yan Gao, Jingjing Meng, Jin Shang, and Yi Sun. Learning attribute and class-specific representation duet for fine-grained fashion analysis. In *CVPR 2023*, 2023. 1, 3
- [22] Yushi Jing, David Liu, Dmitry Kislyuk, Andrew Zhai, Jiajing Xu, Jeff Donahue, and Sarah Tavel. Visual search at pinterest. In *Proceedings of the 21th ACM SIGKDD International Conference on Knowledge Discovery and Data Mining*, pages 1889–1898, 2015. 1, 3
- [23] Jeff Johnson, Matthijs Douze, and Hervé Jégou. Billion-scale similarity search with gpus. *IEEE Transactions on Big Data*, 7(3):535–547, 2019. 1, 4
- [24] M. Hadi Kiapour, Xufeng Han, Svetlana Lazebnik, Alexander C. Berg, and Tamara L. Berg. Where to Buy It: Matching Street Clothing Photos in Online Shops. In *2015 IEEE International Conference on Computer Vision (ICCV)*, pages 3343–3351. IEEE, December 2015. ISBN 978-1-4673-8391-2. doi: 10.1109/ICCV.2015.382. 3
- [25] Alexander Kirillov, Eric Mintun, Nikhila Ravi, Hanzi Mao, Chloe Rolland, Laura Gustafson, Tete Xiao, Spencer Whitehead, Alexander C. Berg, Wan-Yen Lo, Piotr Dollár, and Ross Girshick. Segment anything. *arXiv:2304.02643*, 2023. 2
- [26] Jonathan Krause, Michael Stark, Jia Deng, and Li Fei-Fei. 3D Object Representations for Fine-Grained Categorization. In *2013 IEEE International Conference on Computer Vision Workshops*, pages 554–561. IEEE, December 2013. ISBN 978-1-4799-3022-7. doi: 10.1109/ICCVW.2013.77. 3
- [27] Ananya Kumar, Aditi Raghunathan, Robbie Matthew Jones, Tengyu Ma, and Percy Liang. Fine-tuning can distort pretrained features and underperform out-of-distribution. In *International Conference on Learning Representations*, 2022. 6
- [28] Julia Lasserre, Katharina Rasch, and Roland Vollgraf. Studio2Shop: from studio photo shoots to fashion articles. In *Proceedings of the 7th International Conference on Pattern Recognition Applications and Methods*, pages 37–48, 2018. doi: 10.5220/0006544500370048. 3
- [29] Junnan Li, Dongxu Li, Silvio Savarese, and Steven Hoi. Blip-2: Bootstrapping language-image pre-training with frozen image encoders and large language models. *arXiv preprint arXiv:2301.12597*, 2023. 6, 15
- [30] Shilong Liu, Zhaoyang Zeng, Tianhe Ren, Feng Li, Hao Zhang, Jie Yang, Chunyuan Li, Jianwei Yang, Hang Su, Jun Zhu, et al. Grounding DINO: Marrying DINO with grounded pre-training for open-set object detection. *arXiv preprint arXiv:2303.05499*, 2023. 2
- [31] Si Liu, Zheng Song, Guangcan Liu, Changsheng Xu, Hanqing Lu, and Shuicheng Yan. Street-to-shop: Cross-scenario clothing retrieval via parts alignment and auxiliary set. In *2012 IEEE Conference on Computer Vision and Pattern Recognition*, pages 3330–3337, 2012. 3
- [32] Ziwei Liu, Ping Luo, Shi Qiu, Xiaogang Wang, and Xiaoou Tang. DeepFashion: Powering Robust Clothes Recognition and Retrieval with Rich Annotations. In *2016 IEEE Conference on Computer Vision and Pattern Recognition (CVPR)*, pages 1096–1104. IEEE, June 2016. ISBN 978-1-4673-8851-1. doi: 10.1109/CVPR.2016.124. 3
- [33] Ilya Loshchilov and Frank Hutter. Decoupled weight decay regularization. In *International Conference on Learning Representations*, 2019. 6

- [34] Gen Luo, Yiyi Zhou, Xiaoshuai Sun, Liujuan Cao, Chenglin Wu, Cheng Deng, and Rongrong Ji. Multi-Task Collaborative Network for Joint Referring Expression Comprehension and Segmentation. In *2020 IEEE/CVF Conference on Computer Vision and Pattern Recognition (CVPR)*, pages 10031–10040. IEEE, June 2020. ISBN 978-1-72817-168-5. doi: 10.1109/CVPR42600.2020.01005. 2
- [35] Zhe Ma, Jianfeng Dong, Zhongzi Long, Yao Zhang, Yuan He, Hui Xue, and Shouling Ji. Fine-grained fashion similarity learning by attribute-specific embedding network. In *Proceedings of the AAAI Conference on Artificial Intelligence*, volume 34, 2020. 3
- [36] Suvir Mirchandani, Licheng Yu, Mengjiao Wang, Animesh Sinha, Wenwen Jiang, Tao Xiang, and Ning Zhang. FaD-VLP: Fashion vision-and-language pre-training towards unified retrieval and captioning. In *Proceedings of the 2022 Conference on Empirical Methods in Natural Language Processing*, pages 10484–10497. Association for Computational Linguistics, December 2022. 2
- [37] Emily Mu and John Gutttag. Conditional Contrastive Networks. In *NeurIPS 2022 First Table Representation Workshop*, 2022. 3
- [38] Jianmo Ni, Gustavo Hernandez Abrego, Noah Constant, Ji Ma, Keith Hall, Daniel Cer, and Yinfei Yang. Sentence-t5: Scalable sentence encoders from pre-trained text-to-text models. In *Findings of the Association for Computational Linguistics: ACL 2022*, pages 1864–1874. Association for Computational Linguistics, May 2022. doi: 10.18653/v1/2022.findings-acl.146. 8
- [39] Maxime Oquab, Timothée Darcet, Theo Moutakanni, Huy V. Vo, Marc Szafraniec, Vasil Khalidov, Pierre Fernandez, Daniel Haziza, Francisco Massa, Alaaeldin El-Nouby, Russell Howes, Po-Yao Huang, Hu Xu, Vasu Sharma, Shang-Wen Li, Wojciech Galuba, Mike Rabbat, Mido Assran, Nicolas Ballas, Gabriel Synnaeve, Ishan Misra, Herve Jegou, Julien Mairal, Patrick Labatut, Armand Joulin, and Piotr Bojanowski. Dinov2: Learning robust visual features without supervision, 2023. 8, 18
- [40] Alec Radford, Jong Wook Kim, Chris Hallacy, Aditya Ramesh, Gabriel Goh, Sandhini Agarwal, Girish Sastry, Amanda Askell, Pamela Mishkin, Jack Clark, et al. Learning transferable visual models from natural language supervision. In *International conference on machine learning*, pages 8748–8763. PMLR, 2021. 2, 4, 7
- [41] Raymond Shiao, Hao-Yu Wu, Eric Kim, Yue Li Du, Anqi Guo, Zhiyuan Zhang, Eileen Li, Kunlong Gu, Charles Rosenberg, and Andrew Zhai. Shop The Look: Building a Large Scale Visual Shopping System at Pinterest. In *Proceedings of the 26th ACM SIGKDD International Conference on Knowledge Discovery & Data Mining*, pages 3203–3212, August 2020. doi: 10.1145/3394486.3403372. 1, 3
- [42] Leslie N Smith. Cyclical learning rates for training neural networks. In *2017 IEEE winter conference on applications of computer vision (WACV)*, pages 464–472. IEEE, 2017. 6
- [43] Kihyuk Sohn. Improved Deep Metric Learning with Multi-class N-pair Loss Objective. In *Advances in Neural Information Processing Systems*, volume 29. Curran Associates, Inc., 2016. 4
- [44] Hyun Oh Song, Yu Xiang, Stefanie Jegelka, and Silvio Savarese. Deep Metric Learning via Lifted Structured Feature Embedding. In *2016 IEEE Conference on Computer Vision and Pattern Recognition (CVPR)*, pages 4004–4012. IEEE, June 2016. ISBN 978-1-4673-8851-1. doi: 10.1109/CVPR.2016.434. 3
- [45] Son Tran, R. Manmatha, and C. J. Taylor. Searching for fashion products from images in the wild. In *KDD 2019 Workshop on AI for Fashion*, 2019. 3
- [46] Andreas Veit, Serge Belongie, and Theofanis Karaletsos. Conditional similarity networks. In *Proceedings of the IEEE conference on computer vision and pattern recognition*, pages 830–838, 2017. 3
- [47] Catherine Wah, Steve Branson, Peter Welinder, Pietro Perona, and Serge Belongie. The Caltech-UCSD Birds-200-2011 Dataset. Technical Report CNS-TR-2011-001, California Institute of Technology, 2011. 3
- [48] Xi Wang, Zhenfeng Sun, Wenqiang Zhang, Yu Zhou, and Yu-Gang Jiang. Matching User Photos to Online Products with Robust Deep Features. In *Proceedings of the 2016 ACM on International Conference on Multimedia Retrieval*, pages 7–14. ACM, June 2016. ISBN 978-1-4503-4359-6. doi: 10.1145/2911996.2912002. 3
- [49] Hui Wu, Yupeng Gao, Xiaoxiao Guo, Ziad Al-Halah, Steven Rennie, Kristen Grauman, and Rogerio Feris. Fashion IQ: A New Dataset Towards Retrieving Images by Natural Language Feedback. In *CVPR*, 2019. 3
- [50] Jiannan Wu, Yi Jiang, Peize Sun, Zehuan Yuan, and Ping Luo. Language as Queries for Referring Video Object Segmentation. In *2022 IEEE/CVF Conference on Computer Vision and Pattern Recognition (CVPR)*, pages 4964–4974. IEEE, June 2022. ISBN 978-1-66546-946-3. doi: 10.1109/CVPR52688.2022.00492. 2

- [51] Fan Yang, Ajinkya Kale, Yury Bubnov, Leon Stein, Qiaosong Wang, Hadi Kiapour, and Robinson Piramuthu. Visual Search at eBay. In *Proceedings of the 23rd ACM SIGKDD International Conference on Knowledge Discovery and Data Mining*, pages 2101–2110, August 2017. doi: 10.1145/3097983.3098162. 3
- [52] Licheng Yu, Jun Chen, Animesh Sinha, Mengjiao Wang, Yu Chen, Tamara L Berg, and Ning Zhang. Commercem: Large-scale commerce multimodal representation learning with omni retrieval. In *Proceedings of the 28th ACM SIGKDD Conference on Knowledge Discovery and Data Mining*, pages 4433–4442, 2022. 2, 3
- [53] Yifei Yuan and Wai Lam. Conversational Fashion Image Retrieval via Multiturn Natural Language Feedback. In *Proceedings of the 44th International ACM SIGIR Conference on Research and Development in Information Retrieval (SIGIR '21)*, June 2021. 3
- [54] Yan Zeng, Xinsong Zhang, and Hang Li. Multi-Grained Vision Language Pre-Training: Aligning Texts with Visual Concepts. In *Proceedings of the 39th International Conference on Machine Learning*, pages 25994–26009. PMLR, June 2022. 2
- [55] Yan Zeng, Xinsong Zhang, Hang Li, Jiawei Wang, Jipeng Zhang, and Wangchunshu Zhou. X²-VLM: All-in-one pre-trained model for vision-language tasks. *arXiv preprint arXiv:2211.12402*, 2022. 2
- [56] Andrew Zhai, Hao-Yu Wu, Eric Tzeng, Dong Huk Park, and Charles Rosenberg. Learning a unified embedding for visual search at pinterest. In *Proceedings of the 25th ACM SIGKDD International Conference on Knowledge Discovery & Data Mining*, pages 2412–2420, 2019. 3
- [57] Xunlin Zhan, Yangxin Wu, Xiao Dong, Yunchao Wei, Minlong Lu, Yichi Zhang, Hang Xu, and Xiaodan Liang. Product1M: Towards Weakly Supervised Instance-Level Product Retrieval via Cross-Modal Pretraining. In *2021 IEEE/CVF International Conference on Computer Vision (ICCV)*, pages 11762–11771. IEEE, October 2021. ISBN 978-1-66542-812-5. doi: 10.1109/ICCV48922.2021.01157. 2, 3
- [58] Yanhao Zhang, Pan Pan, Yun Zheng, Kang Zhao, Yingya Zhang, Xiaofeng Ren, and Rong Jin. Visual Search at Alibaba. In *Proceedings of the 24th ACM SIGKDD International Conference on Knowledge Discovery & Data Mining*, pages 993–1001, July 2018. doi: 10.1145/3219819.3219820. 3
- [59] Yuting Zhang, Luyao Yuan, Yijie Guo, Zhiyuan He, I-An Huang, and Honglak Lee. Discriminative Bimodal Networks for Visual Localization and Detection with Natural Language Queries. In *2017 IEEE Conference on Computer Vision and Pattern Recognition (CVPR)*, pages 1090–1099. IEEE, July 2017. ISBN 978-1-5386-0457-1. doi: 10.1109/CVPR.2017.122. 2
- [60] Xiaoyang Zheng, Zilong Wang, Ke Xu, Sen Li, Tao Zhuang, Qingwen Liu, and Xiaoyi Zeng. MAKE: Vision-Language Pre-training based Product Retrieval in Taobao Search. In *Companion Proceedings of the ACM Web Conference 2023*, pages 356–360, April 2023. doi: 10.1145/3543873.3584627. 2, 3
- [61] Mingchen Zhuge, Dehong Gao, Deng-Ping Fan, Linbo Jin, Ben Chen, Haoming Zhou, Minghui Qiu, and Ling Shao. Kaleido-BERT: Vision-Language Pre-training on Fashion Domain. In *2021 IEEE/CVF Conference on Computer Vision and Pattern Recognition (CVPR)*, pages 12642–12652. IEEE, June 2021. ISBN 978-1-66544-509-2. doi: 10.1109/CVPR46437.2021.01246. 2

Appendix

A Dataset

A.1 Samples




IMAGES		
CATEGORY	Head	Head
LAION	BULLDOG HAT - Bonnet - black	Topshop - PLEATED [...] - Haaraccessoire - blue
BLIP2	a black beanie with a stuffed bulldog embroidered on it	an image of a headband with blue color
IMAGES		
CATEGORY	Outwear	Outwear
LAION	Linen trench coat	Unisex Iconic Raincoat Smoking blue
BLIP2	the long coat has been made of blue wool with black detailing	children's rain jacket - navy
IMAGES		
CATEGORY	Bags	Bags
LAION	POPO 22L BACKPACK - Rucksack - vivid purple	Burberry small Banner tote
BLIP2	the purple and blue backpack with straps and compartments	the burberry small leather bag is brown and leather
IMAGES		
CATEGORY	Lower Body	Lower Body
LAION	Y-3 panelled track pants	flared suede trousers
BLIP2	a black sweat jogger pant with pockets	stella pants - dark suede
IMAGES		
CATEGORY	Upper Body	Feet
LAION	DRY TEE TRAIL - Print T-shirt - black	yellow spikaqueen 100 fluorescent leather pumps
BLIP2	nike trail t-shirt in black with the red logo	neon green patent leather heels with studs
IMAGES		
CATEGORY	Upper Body	Neck
LAION	adidas Performance - T-shirt print - tech olive - 4	Codello - STRIPE SCARF - Huiivi - light rose
BLIP2	a adidas 3 stripe green t - shirt	a scarf with multi coloured stripes

Figure 6 – Additional samples from LRV5-F.

A.2 Composition

We classified LRVS-F products into 11 distinct categories. Among these categories, 10 are specifically related to clothing items, which are organized based on their approximate location on the body. Additionally, there is one non-clothing category included to describe some distractors. Tab. 2 provides information regarding the counts of products within each category, as well as the data split. For a more detailed understanding of the clothing categories, Tab. 3 presents examples of fine-grained clothing items that are typically associated with each category.

Each product in our dataset is associated with at least one simple image and one complex image. In Figure 7, we depict the distribution of simple and complex images for each product. Remarkably, we observe that the majority of products, accounting for 90% of the dataset, possess a single simple image and up to four complex images.

	Upper Body	Lower Body	Whole Body	Outwear	Bags	Feet	Neck	Head	Hands	Waist	NonClothing	Total
Train	92 410	75 485	48 446	45 867	26 062	4 224	3 217	1 100	190	184	-	297 185
Val	80	80	80	80	60	6	6	4	2	2	-	400
Test	400	400	400	400	300	30	30	20	10	10	-	2 000
Val. Dist.	19 582	13 488	8 645	6 833	10 274	22 321	2 470	6 003	2 866	1 016	6 043	99 541
Test Dist.	395 806	272 718	172 385	136 062	203 390	448 703	50 881	121 094	57 271	19 853	121 851	2 000 014

Table 2 – Count of simple images (isolated items) across the dataset splits. Some training products are depicted in multiple simple images, hence the total higher than the number of unique identities.

CATEGORY	COMPOSITION
Upper Body	T-shirts, Shirts, Crop Tops, Jumper, Sweater ...
Lower Body	Shorts, Pants, Leggings, Skirts ...
Whole Body	Dress, Gown, Suits, Rompers ...
Outwear	Coat, Jacket ...
Bags	Handbags, Backpack, Luggage ...
Feet	Shoes, Boots, Socks ...
Neck	Scarves, Necklace ...
Head	Hat, Cap, Glasses, Sunglasses, Earrings ...
Hands	Gloves, Rings, Wristbands ...
Waist	Belts

Table 3 – Examples of sub-categories.

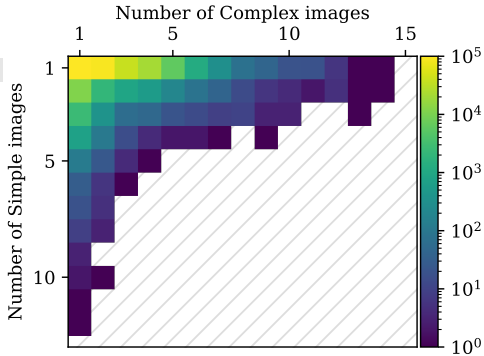


Figure 7 – Distribution of Simple and Complex images across products. 90% of the products have 1 simple image and up to 4 complex images.

B Model

B.1 Retrieval Examples

In this section, we show additional results for our categorical CondViT-B/16 and its textual variant trained with BLIP2[29] captions. We use test query images and the full test gallery with 2M distractors for the retrieval. Each query in the test set is exclusively associated with a single item. However, it should be noted that we do not necessarily query for this item, so the queried product might not be in the gallery. Nevertheless, owing to the presence of 2M distractors, most queries can retrieve multiple viable candidates.

Fig. 8 shows that our categorical CondViT is able to extract relevant features across a wide range of clothing items, and propose a coherent retrieval especially for the main categories. There is still room for improvement on images depicting rare training categories like *Waist*, *Hands*, *Head* or *Neck*, and rare poses.

Fig. 9 presents improvements brought by textual conditioning captions over categorical conditioning. Using text embeddings allows for more natural querying, thanks to the robustness of our model to irrelevant words. However, this robustness comes at the cost of ignoring appearance modifications.

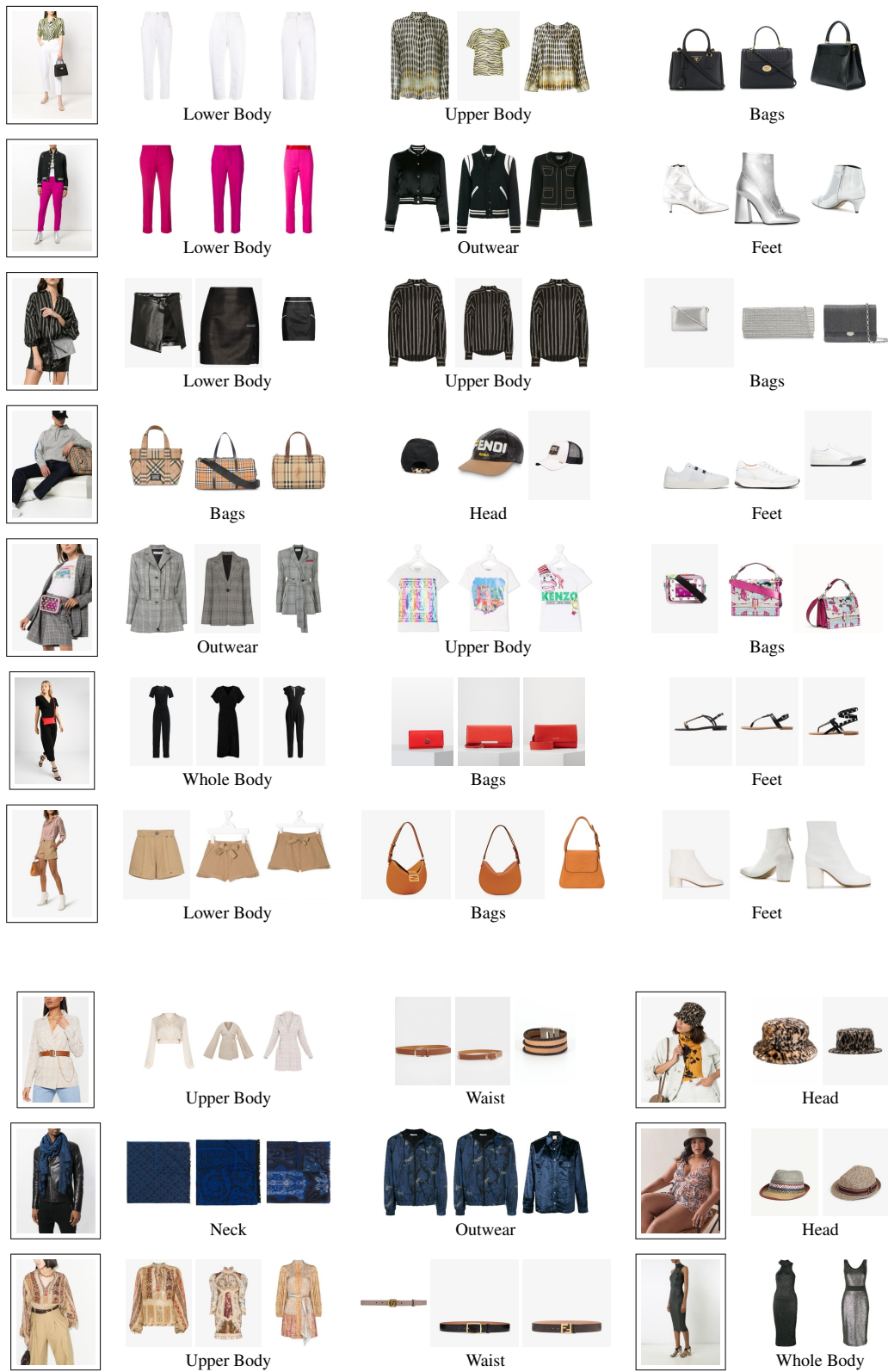
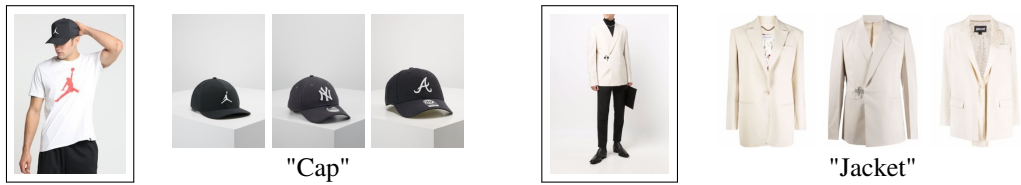


Figure 8 – Qualitative results of our Conditional ViT-B/16 on LRV5-F test set.



(a) Top-3 retrieval for normal user queries. Even though the BLIP2 captions were more detailed, using a single word as a query produces the expected result.



(b) Top-3 retrieval for noisy user queries. Our model is robust to expression of user intent and can focus on the designated object.



(c) Top-3 retrieval for queries with item modifications. In some circumstances, a textual query can influence the result to slightly modify the type of retrieved items, e.g. exchanging shorts and pants or skirts and dresses.



(d) Top-3 retrieval for out-of-frame items. If the network fails, we find that precisizing the query can help.

Figure 9 – Retrieved items for queries in LRVS-F test set with our textual CondViT-B/16. (a) shows results for normal, concise use. (b) shows results with more verbose queries. (c) shows queries influencing the type of results. (d) show results for out-of-frame items.

B.2 Attention Maps

We propose a visualization of the attention maps of our ViT-B/16, ASEN, and our categorical CondViT-B/16 in Fig. 10. We compare attention in the last layer of the transformers with the Spatial Attention applied at the end of ASEN’s global branch. We observe that the attention mechanism in the transformers exhibits a notably sparse nature, selectively emphasizing specific objects within the input scene. Conversely, ASEN demonstrates a comparatively less focused attention distribution. These findings corroborate our earlier qualitative observations, where the unconditional ViT exhibits a pronounced focus on a single object within the scene, while the attention of the CondViT dynamically adjusts in response to the conditioning information.

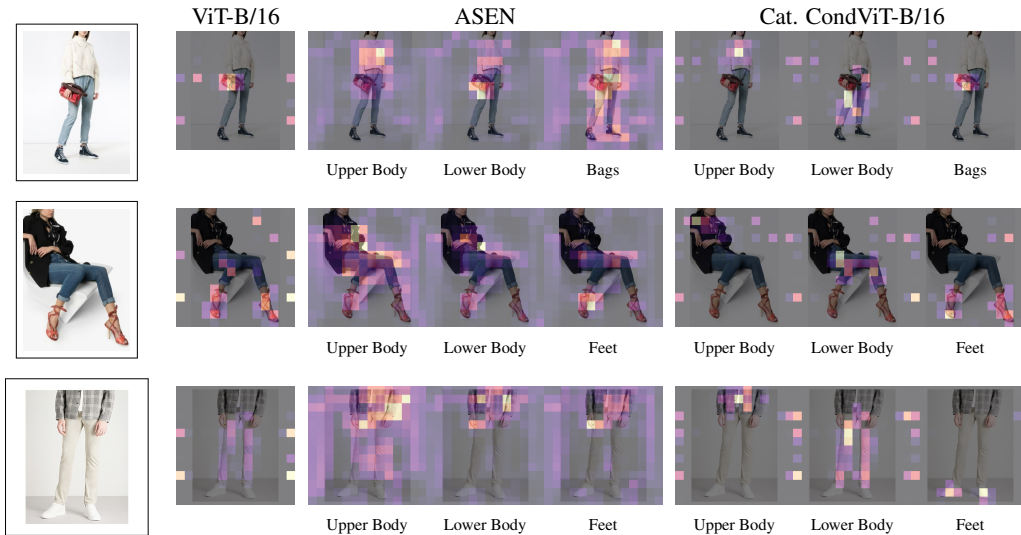


Figure 10 – Attention maps. For ViT-B/16 and CondViT-B/16, we display the maximum attention from the CLS token to the image tokens across all heads in the last layer, and observe sparse maps. For ASEN, we display the attention returned by the Spatial Attention module of the global branch, and observe more diffuse maps. All maps are normalized to [0-1].



Figure 11 – Visualization of the thresholded first component of image tokens in our CondViT-B/16. This component enables separation of the background, foreground, and focused object.

We also visualize the patch features extracted by our models with principal component analysis (PCA) computed on all image tokens in the last layer of our CondViT-B/16 model across the test queries. Similarly to Oquab et al. [39], we find that applying a threshold on the first component enables effective separation of the background from the foreground. Intriguingly, we observe that employing a higher threshold not only accomplishes the aforementioned separation but also yields cleaner visualizations by isolating the conditionally selected object. We also observe instances where the network encounters difficulties in detecting the referenced object, resulting in a notable absence of tokens surpassing the established threshold.

B.3 Ablation Studies

Insertion Depth. We study the impact of the insertion depth of our additional conditioning token by training a series of CondViT-B/32, concatenating the conditioning token before different encoder blocks for each one of them.

Fig. 12 indicates that early concatenation of the conditioning token is preferable, as we observed a decrease in recall for deep insertion (specifically, layers 10-12). However, there was no statistically significant difference in performance between layers 1-8. Consequently, we decided to concatenate the token at the very beginning of the model. We hypothesize that the presence of residual connections in our network enables it to disregard the conditioning token until it reaches the optimal layer. The choice of this layer may depend on factors such as the size of the ViT model and the characteristics of the dataset being used.

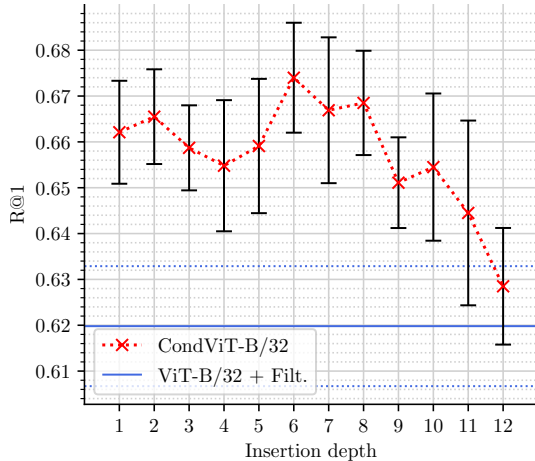


Figure 12 – R@1 on the test set with respect to the insertion depth of the conditioning token. Error bars represent the bootstrapped estimation of the standard deviation across 10 splits. Late insertion degrades performance, but no significant difference can be seen among the first layers.

Asymmetric Conditioning. We experiment with using conditioning for the simple images too, using a single learned "empty" token for all the simple images. We denote this token c_\emptyset . Then for each simple image x_s we compute its embedding as $\phi(x_s, c_\emptyset)$.

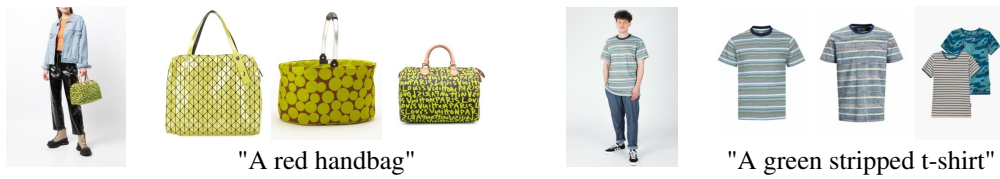
Results in Tab. 4 show that there is no really significant difference between both approaches, even though CondViT-B/16 results are better without this additional token for large amounts of distractors ($\geq 100K$). We choose to keep an asymmetric embedding process.

Distractors →	+0		+10K		+100K		+1M		+2M	
Model	%R@1	%Cat@1	%R@1	%Cat@1	%R@1	%Cat@1	%R@1	%Cat@1	%R@1	%Cat@1
CondViT-B/32	97.0 ±0.57	100 ±0.07	90.9 ±0.98	99.2 ±0.31	80.2 ±1.55	98.8 ±0.39	65.8 ±1.42	98.4 ±0.65	59.0	98.0
CondViT-B/32 + c_\emptyset	96.8 ±0.94	100 ±0.10	91.1 ±1.04	99.3 ±0.24	79.9 ±1.35	99.0 ±0.21	66.0 ±1.36	98.3 ±0.46	59.6	98.2
CondViT-B/16	97.7 ±0.21	99.8 ±0.12	93.3 ±1.04	99.5 ±0.25	85.6 ±1.06	99.2 ±0.35	74.2 ±1.82	99.0 ±0.42	68.4	98.8
CondViT-B/16 + c_\emptyset	97.8 ±0.32	99.9 ±0.11	93.2 ±0.79	99.5 ±0.16	84.4 ±1.16	99.0 ±0.29	72.5 ±1.88	98.8 ±0.42	66.5	98.0

Table 4 – Comparison of symmetric and asymmetric conditioning on LRV5-F test set. We report bootstrapped mean and standard deviation on the test set. There is no significant difference between the configurations. Bold results indicate a difference of more than 1%.

B.4 Textual Conditioning — Failure Cases

We finally present limitations of our textual CondViT-B/16 in Fig. 13. Firstly, when faced with failure in identifying the referenced object, our model resorts to selecting the salient object instead. Additionally, our model ignores queries with color or texture modifications, returning objects as depicted in the query image.



(a) Top-3 retrieval for queries trying to modify color of an item. We find such modifications to be mostly ignored by the model.



(b) Top-3 retrieval for missed queries. For hard queries, or queries about an item not represented in the picture we find a tendency to default to the salient item in the image.

Figure 13 – Retrieved items showing failure cases of our textual CondViT-B/16. (a) shows that the network disregards color clues. (b) shows that the network defaults to the salient item when the query is too hard or not represented.